PRAMANA
— journal of
physics

© Indian Academy of Sciences

Vol. 83, No. 6
December 2014
pp. 985–994

Measurement of nonlinear refractive index in open-aperture *Z*-scan experiments

RITWICK DAS* and MUKESH KUMAR SHUKLA
School of Physical Sciences, National Institute of Science Education and Research, Bhubaneswar 751 005, India
*Corresponding author. E-mail: ritwick.das@niser.ac.in

MS received 7 October 2013; revised 25 February 2014; accepted 4 March 2014
DOI: 10.1007/s12043-014-0819-1; ***e*Publication:** 28 September 2014

Abstract. We present an experimental study on measurement of nonlinear refractive index (n_2) of organic liquids when the thermo-optic effects manifest into large nonlinear phase shifts ($\Delta\phi_0$) in an open-aperture Z-scan configuration. Although we do not obtain the familiar peak–valley normalized transmittance curve as in the case of closed-aperture Z-scan technique, we use a theoretical model using Gaussian beam decomposition (GD) technique to estimate the value of n_2. Using this recipe, we obtain the nonlinear refractive index $n_2 = -(4.90 \pm 1.20) \times 10^{-15}$ cm^2/W for toluene (organic solvent) and $n_2 = -(10.60 \pm 2.10) \times 10^{-15}$ cm^2/W for an organic polymer solution (10^{-4} M in toluene). By carrying out absorption measurements directly with an unfocussed Gaussian beam, we found nonlinear absorptions $\beta_{\text{tol}} = (2.42 \pm 0.20) \times 10^{-13}$ m/W and $\beta_{\text{poly}} = (2.79 \pm 0.24) \times 10^{-13}$ m/W which are close to the expected results.

Keywords. Nonlinear refractive index; nonlinear phase; Gaussian beam.

PACS Nos 42.70.Mp; 42.65.Hw

1. Introduction

The simplicity and high sensitivity of Z-scan technique using a single beam to measure the nonlinear refractive index (n_2) and nonlinear absorption coefficient (β) makes it arguably the most convenient experiment to estimate the nonlinear optical properties of solids as well as liquids [1,2]. Fundamentally, the induced phase shift (attenuation) in focussed Gaussian beam due to optical nonlinearity of the medium, forms the basis of closed-aperture (or open-aperture) Z-scan technique [2,3]. In order to ascertain the nonlinear optical (NLO) parameters when the induced phase shift (attenuation) is small, the closed (or open) aperture transmittance is analysed using the Gaussian decomposition (GD) technique as a first-order approximation [2–5]. Consequently, we obtain convenient analytical expressions relating the normalized transmittance (T) at far-field to n_2 and β [1–8]. On the other hand, it is crucial to appreciate that the non-resonant nonlinear

responses are extremely fast (≈ a few femtosecond) and therefore, require ultrashort pulses for appropriate characterization of NLO properties [9,10]. Typically, such lasers have high repetition rates (>1 MHz) which can lead to thermal lensing as a consequence of accumulated thermal effects (ATE) [11–14]. The ATE comes into play when pulses are incident on a time-scale faster than the characteristic thermal lifetime $t_c = w_0^2/4D$ where w_0 is the beam-spot size and D is the thermal diffusivity of the medium [11]. This manifestation is prominent in liquids due to their small thermal diffusivities (10^{-7}–10^{-8} m^2/s) as compared to solid dielectrics such as quartz (10^{-4}–10^{-5} m^2/s). Hence, it is expected that the overestimation of NLO properties using such ultrafast laser sources would be more in liquids. In the present work, we study the open-aperture normalized transmittance of organic solutions when $\Delta\phi_0$ is significantly large and employ the higher-order terms in the GD method to obtain nonlinear refractive index (n_2).

2. Experimental set-up and results

The Z-scan set-up shown in figure 1 comprises a femtosecond (fs) Yb-fibre laser, delivering linearly polarized pulses of 250 fs at 80 MHz repletion rate at 1064 nm wavelength with a maximum average output power of 5.0 W. We use a combination of half-wave plate (HWP) and polarizing beam splitter (PBS) to vary the optical power to be incident on the sample. Importantly, the fibre laser architecture ensures that the output power is delivered in TEM_{00} mode and our beam profile measurement gives $M^2 < 1.08$ ensuring a good-quality Gaussian beam profile. The output pulses were focussed using a converging lens ($f = 200$ mm) resulting in a beam waist of $w_0 = 75.0 \pm 1.0$ μm and hence, on-axis peak irradiances vary between $I_0 = 0.10$ GW/cm^2 and $I_0 = 1.0$ GW/cm^2 at the focal point. We used toluene and a pi-conjugated organic polymer solution (10^{-4} M in toluene) as samples [9]. A 1.0 mm (L) thick glass cuvette carrying the liquid samples were mounted on a motorized translation stage of 10.0 cm travel. The organic polymer solution, namely 5,10,15-Tris[3,4-(1,4-dioxan)phenyl]corrole, is expected to exhibit slightly strong NLO behaviour compared to toluene [15]. Although the closed-aperture Z-scan response has

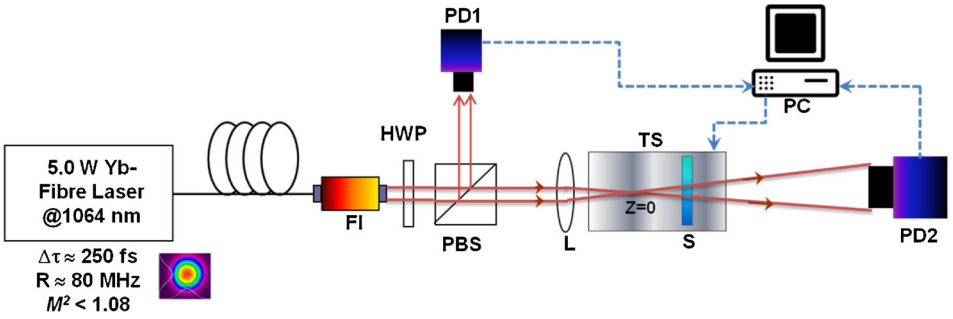

Figure 1. Experimental set-up for open-aperture Z-scan measurement using Yb-fibre laser source. FI: Faraday isolator; HWP: half-wave plate; PBS: polarizing beam-splitter; L: lens ($f = 100$ mm); TS: translation stage (10 cm travel); S: sample; PD1: reference photodetector; PD2: signal photodetector.

been reported elsewhere [15], the NLO properties of this polymer in an open-aperture configuration has not been investigated previously. The transmitted power was detected using two different photodetectors (3A-P-Ophir and 8180P-001-12-Newport) and a compatible power meter. The diameter of the active area for both the photodetectors was 12.0 mm.

Figures 2a and 2b show the measured normalized transmittance of toluene and organic polymer solution respectively for different incident optical power (dotted curves). The black, blue, green and brown dots (experimental) correspond to $I_0 = 0.50$ GW/cm^2, 0.70 GW/cm^2, 0.85 GW/cm^2 and 1.00 GW/cm^2 respectively. The curve represents fall in transmission close to $z = 0.0$ mm. Also, we recorded the beam intensity profiles of the transmitted beam using a CCD camera (GRAS-50S5M-C, Point-Grey Inc.) for toluene when the sample is scanned along z. The CCD camera has an approximate active area of 8.0 mm $\times$ 7.5 mm with 3.45 μm pixel size. A planoconvex lens of 500 mm focal length was placed at about 60 mm from the point $z = 0$ in figure 1 for capturing the beam intensity profiles on CCD camera. The recorded beam intensity profiles is shown in figure 3a at points $z = -50.0$ mm, -25.0 mm, 0.0 mm and 35.0 mm (of figure 2a) for an on-axis peak irradiance of $I_0 = 0.50$ GW/cm^2. By keeping in mind the variation of normalized transmittance in a closed-aperture Z-scan case with negative n_2, the beam intensity distribution at $z = -50.0$ mm (far-from-focus), -25.0 mm (peak), 35.0 mm (far-from-focus) is expected. However, the beam intensity distribution at $z = 0.0$ mm is significantly broader as compared to active area of the camera. Consequently, if we assume that the CCD camera is replaced by a photodetector with $\sim$10.0 mm active diameter, optical power in the transmitted beam is measured partially if the active area of photodetector is smaller than the cross-sectional area of the transmitted Gaussian beam. This situation becomes highly probable in case of large $\Delta\phi_0$ ($\gg \pi$). Therefore, in an open-aperture Z-scan measurement, the valley depicting the phenomenon of absorption can be a consequence of large nonlinear refraction which makes the beam spread beyond the detector's active area. For comparison with low on-axis peak irradiances, we recorded the beam profiles at identical points in Z-scan for $I_0 = 0.10$ GW/cm^2 which is shown in figure 3b. From the beam profile at $z = 0$, it is evident that such wide spreading of beam is not observed in this case. By repeatedly carrying out the Z-scan, we have observed that point $z = 0.0$ mm (figure 2a) is slightly shifted towards the right ($\sim$4.0$-$5.0 mm) of the focal point of the lens. This pertains to a situation when the beam is incident from the left. Therefore, assuming that such a behaviour is due to nonlinear refraction, the post-focal minima in normalized transmittance curve (figure 2a) imply a negative value for n_2. An alternate argument behind such an observation was theoretically proposed by Chen *et al* [3] by comparing the radial distribution of field patterns at peak, valley and far-from-focus (linear) points in the normalized transmittance curve. The measured beam profiles in figures 3a and 3b give experimental proofs to their argument. It can be easily ascertained from figure 3a that the Gaussian-field pattern undergoes discernible change between peak ($z = -25.0$ mm), valley ($z = 0.0$ mm) and far-from-focus ($z = -50.0$ mm and $z = 35.0$ mm) points when $\Delta\phi_0 > \pi$. At far-from-focus points ($z = -50.0$ mm and 35.0 mm), the optical transverse beam profile preserves its Gaussian shape. At the peak ($z = -25.0$ mm), the Gaussian beam shape is preserved but the shape is significantly narrower (along x and y) as compared to far-from-focus points. On the other hand, the transverse beam profile at the valley ($z = 0.0$ mm) is very flat and does not

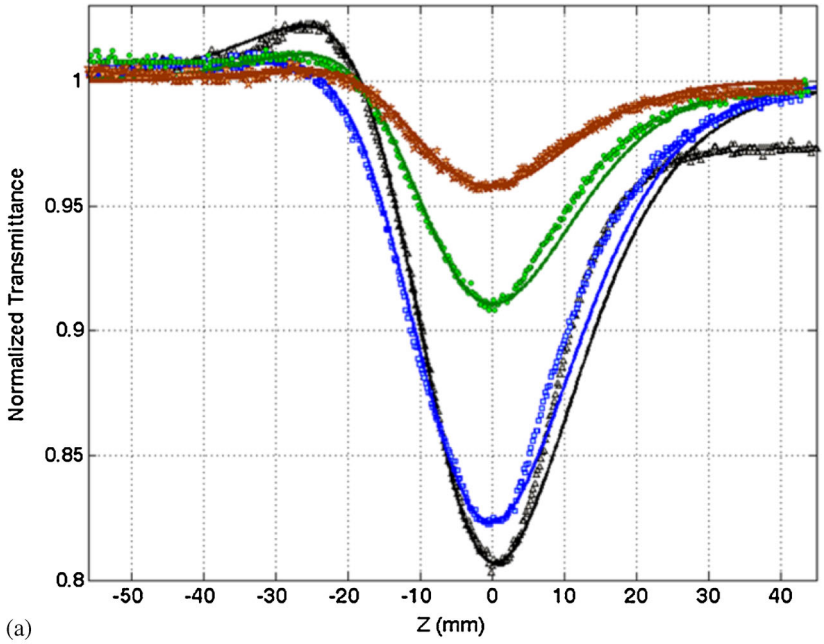

(a)

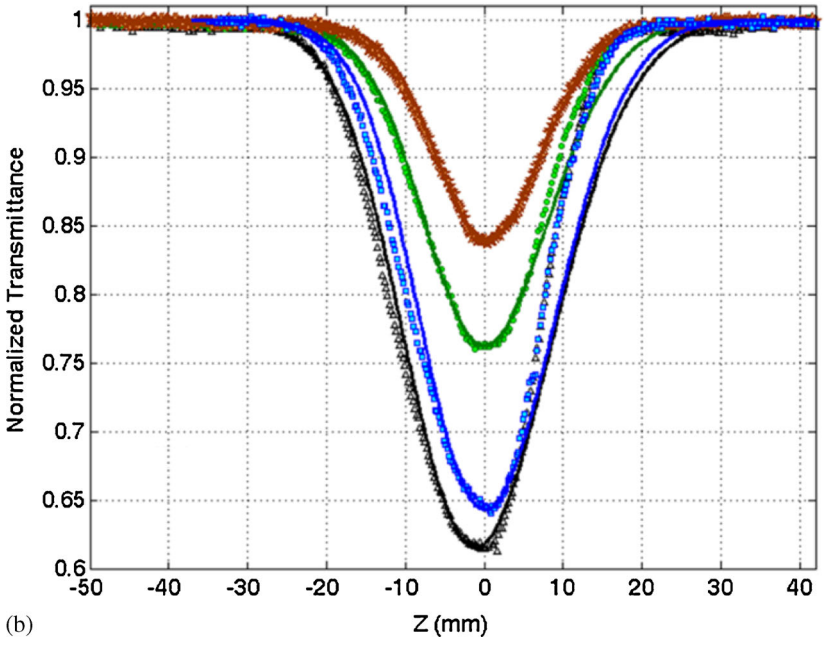

(b)

Figure 2. (**a**) Open-aperture normalized transmittance curve for toluene for $I_0 = 0.50$ GW/cm^2, 0.70 GW/cm^2, 0.85 GW/cm^2 and 1.00 GW/cm^2. (**b**) Open-aperture normalized transmittance curve for organic polymer solution (10^{-4} M in toluene) for $I_0 = 0.50$ GW/cm^2, 0.70 GW/cm^2, 0.85 GW/cm^2 and 1.00 GW/cm^2 (dotted curve – experimental; solid curve – theoretical fit as per eq. (3)).

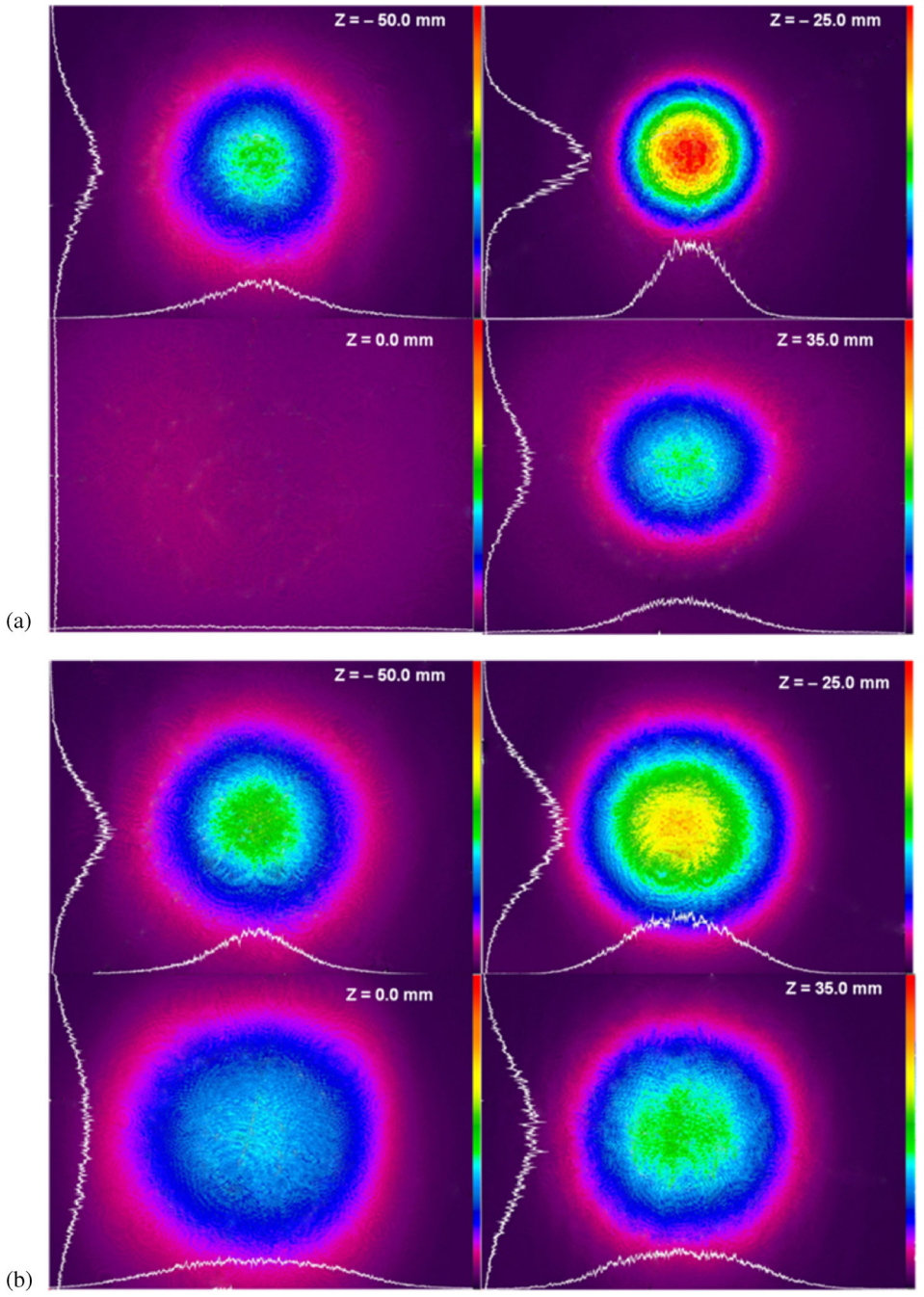

Figure 3. (**a**) Beam intensity profiles at $z = -50.0$ mm, -25.0 mm, 0.0 mm and 35.0 mm at $I_0 = 0.50$ GW/cm^2 for toluene. (**b**) Beam intensity profiles at $z = -50.0$ mm, -25.0 mm, -0.0 mm and 35.0 mm at $I_0 = 0.10$ GW/cm^2 for toluene.

have a Gaussian shape. Therefore, the transmitted beam at the valley is expected to have a smaller magnitude when measured using a photodetector of ∼10.0–12.0 mm active diameter which is a very standard dimension for commercially available photodetectors. This will result in a drop in normalized transmittance as shown in figures 2a and 2b. However, the change in Gaussian-field pattern ($\Delta\phi_0 \ll \pi$, $I_0 = 0.1\,\mathrm{GW/cm^2}$) at peak ($z = -25.0$ mm), valley ($z = 0.0$ mm) and far-from-focus ($z = -50.0$ mm and $z = 35.0$ mm) points in figure 3b is quite small indicating that the transmittance through the sample will not exhibit any valley.

3. Theoretical modelling and estimation of n_2

In view of the recorded beam intensity profiles in figures 3a and 3b, we analyse the normalized transmittance curves using higher-order terms of the GD technique originally proposed by Sheik Bahae *et al* [2]. According to the GD technique, we express the electric field of the beam propagating from exit plane of the medium exhibiting $\chi^{(3)}$ nonlinearity as a sum of multiorder Gaussian beams [2,3],

$$E_a(r,z,t) = E_e(z, r=0, t)\mathrm{e}^{(-\alpha L/2)} \times \sum_{m=0}^{\infty} \frac{[-i\,\Delta\phi_0(z,t)]^m}{m!} \frac{w_{m0}}{w_0} \times \mathrm{e}^{\left(-\frac{r^2}{w_m^2} - \frac{ikr^2}{2R_m} + i\theta_m\right)}, \tag{1}$$

where $\Delta\phi_0(z,t) = \Delta\phi_0(t)/[1+(z/z_r)^2]$, $\Delta\phi_0(t) = k_0(n_0 - n_2 I_0)L_{\mathrm{eff}}$ in on-axis phase-shift at focus, $L_{\mathrm{eff}} = (1-\mathrm{e}^{\alpha L})/\alpha$; L is the sample length, α is the linear absorption coefficient, n_0 is the linear refractive index, n_2 is the nonlinear refractive index, $k_0 = 2\pi/\lambda$ and λ is the laser wavelength. E_e is the on-axis field of the laser pulse at the exit plane of the sample. If d is defined as the free-space propagation distance from the centre of the medium to the aperture plane, then [3]

$$w_{m0}^2 = \frac{w^2(z)}{(2m+1)}, \quad d_m = (1/2)kw_{m0}^2, \quad R_m = \frac{d}{[1 - g/(g^2 + d^2/d_m^2)]},$$

$$\theta_m = \tan^{-1}\left[\frac{(d/d_m)}{g}\right], \quad w_m^2 = w_{m0}^2\left(g^2 + \frac{d^2}{d_m^2}\right).$$

Also,

$$w(z) = \frac{w_0}{[1+(z/z_r)^2]^{1/2}},$$

where w_0 is the beam-waist radius (at $z = 0$),

$$R(z) = z[1 + (z_r/z)^2]^{1/2}$$

is the wave-front radius at z, $z_r = \frac{1}{2}k_0 w_0^2$ is the diffraction length and

$$g = 1 + \frac{d}{R(z)}.$$

Here m defines the order of Gaussian beam decomposition and for small phase shift ($\Delta\phi_0 < \pi$), $m = 1$ leads to on-axis normalized transmittance through the sample which is given by [16]

$$T(z) = 1 + \frac{4(z/z_r)\Delta\phi_0}{(z^2/z_r^2 + 1)(z^2/z_r^2 + 9)}. \tag{2}$$

For an aperture of radius r_a, the transmittance through the aperture is characterized in terms of the difference between peak and valley of T curve as $T_{p-v} = 0.405(1-S)^{0.27}\Delta\phi_0$ where S is the linear aperture transmittance [1,2]. However, when $\Delta\phi_0 > \pi$ or $S > 0.70$, we consider the formulation proposed by Chen *et al* [3] where higher-order terms in the GD method have been considered to estimate sample transmission. In that case, the normalized transmittance is given by [3]

$$T_N = \frac{1}{S}\sum_{m=0}^{\infty}\sum_{n=0}^{\infty} p_{mn}\left[\cos\left(\alpha_{mn}\frac{\pi}{2}\right) - \exp(-q_{mn}Y_a^2)\cos\left(\alpha_{mn}\frac{\pi}{2} - r_{mn}Y_a^2\right)\right], \tag{3}$$

where

$$Y_a\left(= \frac{(r_a z_r)}{(d w_0)} = \left[-\frac{1}{2}\ln(1-S)\right]^{1/2}\right)$$

is the ratio of the aperture radius (r_a) to Gaussian beam radius (w_0) at the aperture plane. Also,

$$\alpha_{mn} = m - n, \quad p_{mn} = \left[\Delta\phi_0/(1 + z^2/z_r^2)\right]^{(m+n)}\left[\frac{1}{\{m!n!(m+n+1)\}}\right],$$

$$q_{mn} = \left[1 + z^2/z_r^2\right]\left[\frac{2m+1}{z^2/z_r^2 + (2m+1)^2} + \frac{2n+1}{z^2/z_r^2 + (2n+1)^2}\right]$$

and

$$r_{mn} = \left[\frac{4(z/z_r)(z^2/z_r^2 + 1)(m-n)(m+n+1)}{\{z^2/z_r^2 + (2m+1)^2\}\{z^2/z_r^2 + (2n+1)^2\}}\right].$$

It is interesting to note that, for $\Delta\phi_0 \geq \pi$, the peak of the normalized transmittance reduces with respect to the valley when $S > 0.80$ and the peak almost vanishes when $S \geq 0.98$–0.99. This is primarily due to $1/S$ dependence of the normalized transmittance in eq. (3) which leads to a drop in T_N for large $\Delta\phi_0$. The variation of normalized transmittance in our open-aperture measurements resembles such a behaviour and hence, using the expression for T_N in eq. (3), we theoretically fit the experimental data in figures 2a and 2b (solid lines) for $S > 0.99$. As expected, the peaks in normalized transmittance curve vanish as $S \sim 0.99$ ($Y_a > 1.50$) for $\Delta\phi_0 \gg \pi$. Also, we obtain the average value of nonlinear refractive index, $n_2 = -(4.90 \pm 1.20) \times 10^{-15}$ cm^2/W for toluene and $n_2 = -(10.6 \pm 2.10) \times 10^{-15}$ cm^2/W for the organic polymer solution. It is worthwhile to note that the measured value of nonlinear refractive index (n_2) for toluene matches closely with the values reported by Gnoli *et al* [12] and Couris *et al* [13].

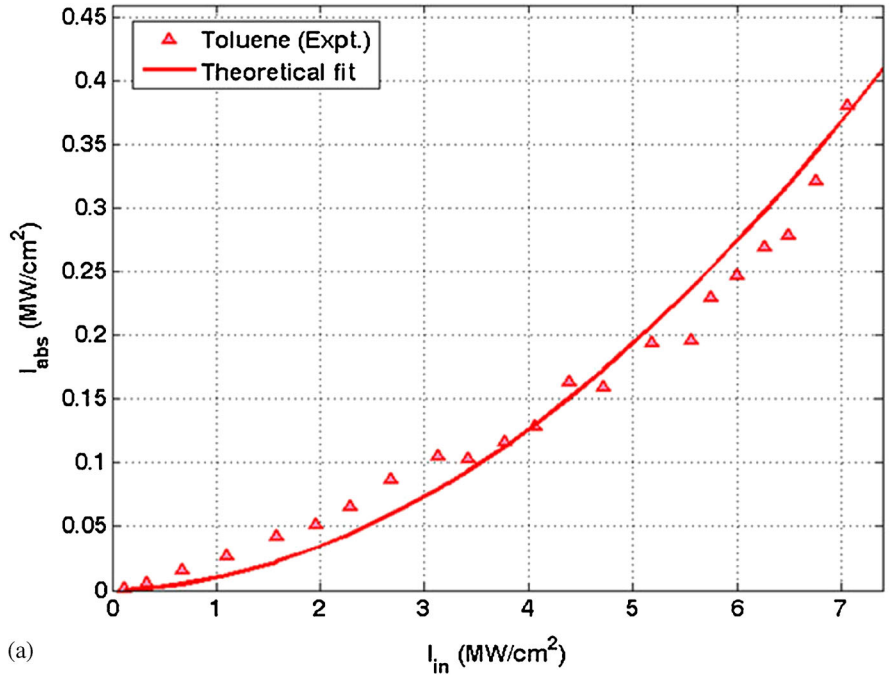

(a)

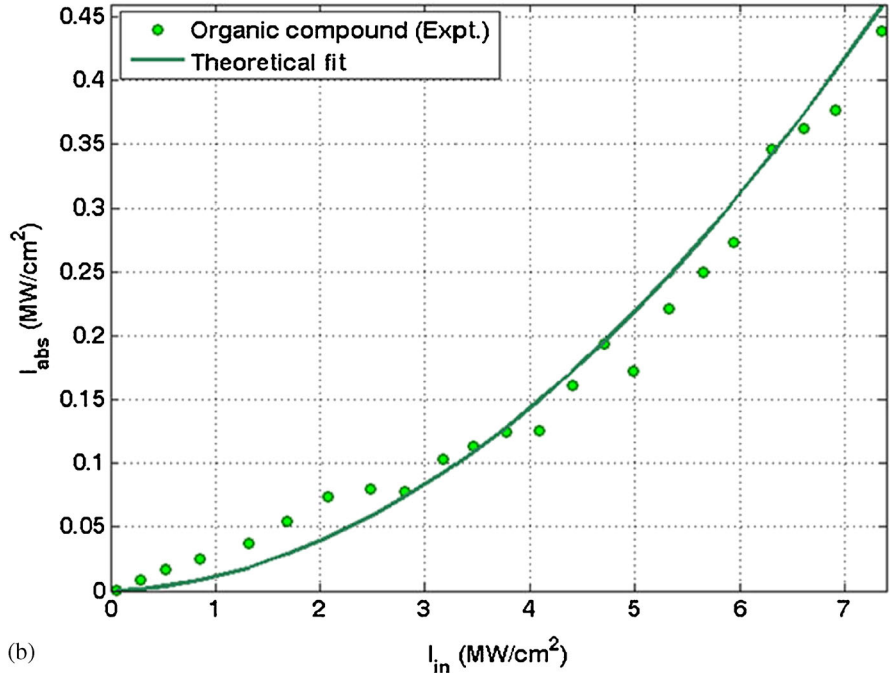

(b)

Figure 4. (**a**) Intensity absorbed (I_{abs}) as a function of incident intensity (I_{in}) for toluene. (**b**) Intensity absorbed (I_{abs}) as a function of incident intensity (I_{in}) for OC solution (in toluene) (dotted curve – experimental; solid curve – theoretical fit).

4. Determination of nonlinear absorption (β)

In order to obtain β, we varied the incident optical intensity (I_0) of an unfocussed beam from the femtosecond pulsed laser and measured the optical absorption of samples (toluene and polymer) as a function of incident intensity. The measured absorbed intensity is shown in figures 4a and 4b respectively. It is evident that the curve exhibits nonlinear behaviour at higher intensities ($I_{\text{in}} \geq 4$ MW/cm^2). Subsequently, we solved the equation $(\mathrm{d}I/\mathrm{d}z) = -\alpha I - \beta I^2$ where α and β are linear and nonlinear absorption coefficients respectively. As a suitable initial condition, we considered $I(z = 0)$ to be the laser fluence per unit area averaged over one thermal time-scale (t_c). The solution is given by

$$I(z = L) = \frac{I(z = 0)\mathrm{e}^{-\alpha L}}{[1 + (\beta/\alpha)\{I(z = 0)\}(1 - \mathrm{e}^{\alpha L})]}. \tag{4}$$

Using the measured beam waist ($w \approx 1.25$ mm) of unfocussed incident beam and $\alpha_{\text{tol}} = 0.216$ cm^{-1} [17], the theoretical fits (solid lines in figures 4a and 4b) result into $\beta_{\text{tol}} = (2.42 \pm 0.20) \times 10^{-13}$ m/W and $\beta_{\text{poly}} = (2.79 \pm 0.24) \times 10^{-13}$ m/W. Although the impact of thermo-optic effects cannot be ignored in our measurements, the estimation of nonlinear absorption coefficient is close to the expected value [12,13].

5. Conclusion

The method and results presented in this work gave rise to the possibility of estimating nonlinear refractive index n_2 in an open-aperture Z-scan configuration when the nonlinear phase shift was large ($\Delta\phi_0 > \pi$). We found that the nonlinear refractive index $n_2 = -(4.90 \pm 1.20) \times 10^{-15}$ cm^2/W for toluene (organic solvent) and $n_2 = -(10.60 \pm 2.10) \times 10^{-15}$ cm^2/W for an organic polymer (5,10,15-Tris[3,4-(1,4-dioxan)phenyl] corrole) solution (10^{-4} M in toluene) which is in close agreement with the values reported in literature. It is important to note that the thermally-induced large nonlinear phase shift is quite probable at high repetition rate (>1 MHz) lasers and therefore, the open-aperture Z-scan measurements can be used for estimating n_2 as well as β by employing appropriate theoretical models such as GD technique. However, in addition to the route described in our work, it is important to obtain the contribution from thermo-optic effects in order to have exact estimation of electronic contribution in closed- as well as open-aperture techniques. The present investigation showed that the role played by aperture size could not be ignored in determining nonlinear optical parameters in an open-aperture Z-scan measurement and the drop in optical transmission could be a consequence of large phase shift due to nonlinear refraction [3]. Recent investigations also revealed that the open-aperture measurements could be accompanied by pseudo-responses from standard materials such as BK7 glass due to changes in incident angle and azimuth polarization angle of the focussed beam [18]. Therefore, it is important to realize that the variation of normalized transmittance in an open-aperture Z-scan configuration could have signatures from various effects such as nonlinear refraction, material dispersion, thermo-optic effects and characteristics of incident beam [11,18–20]. Depending on the impact of such effects on the measurement, the open-aperture Z-scan measurements can be employed for estimating the associated physical quantities such as n_2 in our case.

References

[1] M Sheik-Bahae, A A Said and E W Stryland, *Opt. Lett.* **14**, 955 (1989)
[2] M Sheik-Bahae, A A Said, T Wei, D J Hagan and E W Stryland, *IEEE J. Quantum Electron.* **26**, 760 (1990)
[3] S Q Chen, Z B Liu, W P Zang, J G Tian, W Y Zhou, F Song and C P Zhang, *J. Opt. Soc. Am. B* **22**, 1911 (2005)
[4] J Wei and M Xiao, *J. Opt. A: Pure Appl. Opt.* **10**, 115102 (2008)
[5] Y Chenga, Y Maoa, J Liua, S Fenga and T Hea, *J. Mod. Opt.* **54**, 2763 (2007)
[6] X Liu, S Geo, H Wang, H Wang and L Hou, *Opt. Commun.* **197**, 431 (2009)
[7] T Hea and C Wanga, *J. Mod. Opt.* **55**, 3013 (2008)
[8] G Tsigaridas, I Polyzos, P Persephonis and V Giannetas, *Opt. Commun.* **266**, 284 (2006)
[9] M Samoc, A Samoc, B L Davies, Z Bao, L Yu, B Hsieh and U Scherf, *J. Opt. Soc. Am. B* **15**, 817 (1998).
[10] G L Wood, M J Miller and A G Mott, *Opt. Lett.* **20**, 973 (1995)
[11] M Falconieri, *J. Opt. A: Pure Appl. Opt.* **1**, 662 (1999)
[12] A Gnoli, L Razzari and M Righini, *Opt. Express* **13**, 7976 (2005)
[13] S Couris, M Renard, O Faucher, B Lavorel, R Chaux, E Koudoumas and X Michaut, *Chem. Phys. Lett.* **369**, 318 (2003)
[14] R D Nalda, R D Coso, J R Isidro, J Olivares, A S Garcia, J Solis and C N Afonso, *J. Opt. Soc. Am. B* **19**, 289 (2002)
[15] A Garai, W Sinha, C S Purohit, R Das and S Kar, unpublished work (2014)
[16] B Yao, L Ren and X Hou, *J. Opt. Soc. Am. B* **20**, 12901294 (2003)
[17] S Kedenburg, M Vieweg, T Gissibl and H Giessen, *Opt. Mat. Express* **2**, 1588 (2012)
[18] R Wang, J Wei and M Xiao, *J. Opt.* **15**, 025204 (2013)
[19] Q Lin, J Zhang, G Piredda, R W Boyd, P M Fauchet and G P Agrawal, *Appl. Phys. Lett.* **91**, 021111 (2013)
[20] X L Zhang, Z B Liu, X C Li, Q Ma, X D Chen, J G Tian, Y F Xu and Y S Chen, *Opt. Express* **21**, 7511 (2013)